Supplemental Information to:

High-density cultivation of terrestrial *Nostoc* strains leads to reprogramming of secondary metabolome

Arthur Guljamow, Marco Kreische, Keishi Ishida, Anton Liaimer, Bjørn Altermark, Lars Bähr, Christian Hertweck, Rudolf Ehwald and Elke Dittmann

Table of contents:

Table S1 Adjustment of light intensity and CO_2 supply to increasing cell densities during growth in HD cultivation.

wet weight (g/L)	light intensity over the culture (µmol photons $\cdot s^{-1} \cdot m^{-2}$)	p CO_2 (mbar)
<100	100	32
100 to 150	158	
150 to 200	215	90
200 to 250	330	
250 to 350	440	
>350	560	

Table S2. Three new anabaenopeptins from *N. punctiforme* KVJ2 and the similar congeners.

	Amino acid position						
Peptide	1	2	3	4	5	6	Ref.
Anabaenopeptin KVJ827 (**8**)	L-Tyr	D-Lys	L-Val	L-Hph	MeGly	L-Hph	This study
Anabaenopeptin KVJ841 (**9**)	L-Tyr	D-Lys	L-Ile	L-Hph	MeGly	L-Hph	This study
Anabaenopeptin KVJ811 (**10**)	L-Phe	D-Lys	L-Val	L-Hph	MeGly	L-Hph	This study
Anabaenopeptin NZ825	L-Phe	D-Lys	L-Ile	L-Hph	MeGly	L-Hph	#1
Anabaenopeptin NZ841	L-Phe	D-Lys	L-Ile	L-Hty	MeGly	L-Hph	#1
Anabaenopeptin NZ857	L-Phe	D-Lys	L-Ile	L-Hty	MeGly	L-Hty	#1,2
Nostamide A (**3**)	L-Phe	D-Lys	L-Ile	L-Hph	MeGly	L-Hty	#2

Hph; homophenylalanine, Hty; homotyrosine, MeGly; *N*-methylglycine

#1 Grach-Pogrebinsky O, Carmeli S. Tetrahedron 2008 64, 10233–10238.
#2 Rouhiainen L, Jokela J, Fewer DP, Urmann M, Sivonen K. Chem Biol. 2010 17, 265-273.

Table S3. The ^{1}H and ^{13}C data for anabaenopeptin KVJ827 in DMSO-d_6 at 300 K.

		Isomer1		Isomer2	
Position		^{1}H (*J* Hz)	^{13}C	^{1}H (*J* Hz)	^{13}C
Tyr	1		173.76 (s)		173.83 (s)
	2	4.25 (ddd 16.0, 8.2, 5.2)	54.0 (d)	4.26 (ddd 15.5, 8.3, 5.4)	54.0 (d)
	3	2.74 (m)	36.66 (t)	2.74 (m)	36.66 (t)
		2.85 (m)		2.85 (m)	
	4		127.3 (s)		127.2 (s)
	5,9	6.94 (d 8.5)	130.10 (d)	6.95 (d 8.5)	130.13 (d)
	6,8	6.64 (d 8.5)	115.0 (s)	6.65 (d 8.5)	115.0 (s)
	7		156.0 (s)		156.0 (s)
	NH	6.18 (d 8.2)		6.21 (d 8.3)	
	Ureido C=O		156.97 (s)		157.07 (s)
Lys	1		172.8 (s)		172.1 (s)
	2	3.87 (m)	54.4 (d)	3.87 (m)	54.7 (d)
	3	1.53 (m)	31.1 (t)	1.53 (m)	31.1 (t)
		1.60 (m)		1.60 (m)	
	4	1.08 (m)	20.2 (m)	1.08 (m)	20.8 (m)
		1.17 (m)		1.17 (m)	
	6	1.33 (m)	28.0 (t)	1.33 (m)	28.0 (t)
		1.35 (m)		1.35 (m)	
	7	2.89 (m)	38.2 (t)	2.71 (m)	38.2 (t)
		3.28 (m)		3.43 (m)	
	1-NH	6.50 (m)		6.49 (m)	
	6-NH	7.12 (m)		7.19 (m)	
Val	1		172.5 (s)		171.6 (s)
	2	3.94 (t 7.8)	57.8 (d)	3.79 (t 7.5)	59.1 (d)
	3	1.82 (m)	29.7 (t)	1.85 (m)	29.7 (t)
	4	0.834 (d 6.6)	18.8 (t)	0.80 (d 6.7)	19.1
	5	0.93 (d 6.8)	18.8 (t)	0.828 (d 6.6)	19.0
	NH	6.76 (d 7.2)		7.13 (m)	
Hph1	1		171.2 (s)		171.6 (s)
	2	4.66 (dt 8.6, 5.4)	49.2 (d)	4.46 (br)	49.0 (d)
	3	1.85 (m)	32.8 (t)	1.88 (m)	32.8 (t)
		1.92 (m)			
	4	2.58 (m)	30.9 (t)	2.59 (m)	31.4 (t)
		2.75 (m)		2.64 (m)	
	5		141.2 (s)		141.1 (s)
	6,10	7.21 (m)	128.32 (d)	7.24 (m)	128.17 (d)
	7,9	7.23 (m)	128.23 (d)	7.23 (m)	128.23 (d)
	8	7.17 (m)	125.98 (d)	7.17 (m)	126.00 (d)
	NH	8.90 (d 5.4)		8.25 (br)	
N-MeGly	1		168.4 (s)		168.9 (s)
	2	3.40 (d 16.2)	52.17 (t)	3.62 (d 16.6)	53.9 (t)
		4.43 (d 16.2)		4.57 (d 16.6)	
	N-Me	3.01 (s)	36.8 (q)*	2.81 (s)	33.8 (q)*
			37.0 (q)*		33.9 (q)*
Hph2	1		171.0 (s)		171.0 (s)
	2	4.15 (ddd 10.5, 8.7, 4.6)	52.2 (d)	4.08 (ddd 11.3, 8.6, 3.3)	52.9 (d)
	3	1.77 (m)	33.3 (t)	1.90 (m)	32.5 (t)
		2.10 (m)		2.11 (m)	
	4	2.42 (m)	31.9 (t)	2.45 (m)	31.5 (t)
		2.52 (m)		2.60 (m)	
	5		141.33 (s)		141.25 (s)
	6,10	7.10 (m)	128.32 (d)	7.13 (m)	128.36 (d)
	7,9	7.28 (m)	128.36 (d)	7.28 (m)	128.32 (d)
	8	7.17 (m)	125.8 (d)	7.17 (m)	125.7 (d)
	NH	7.90 (d 8.8)		8.55 (d 8.6)	

**: Two carbons are detected.*

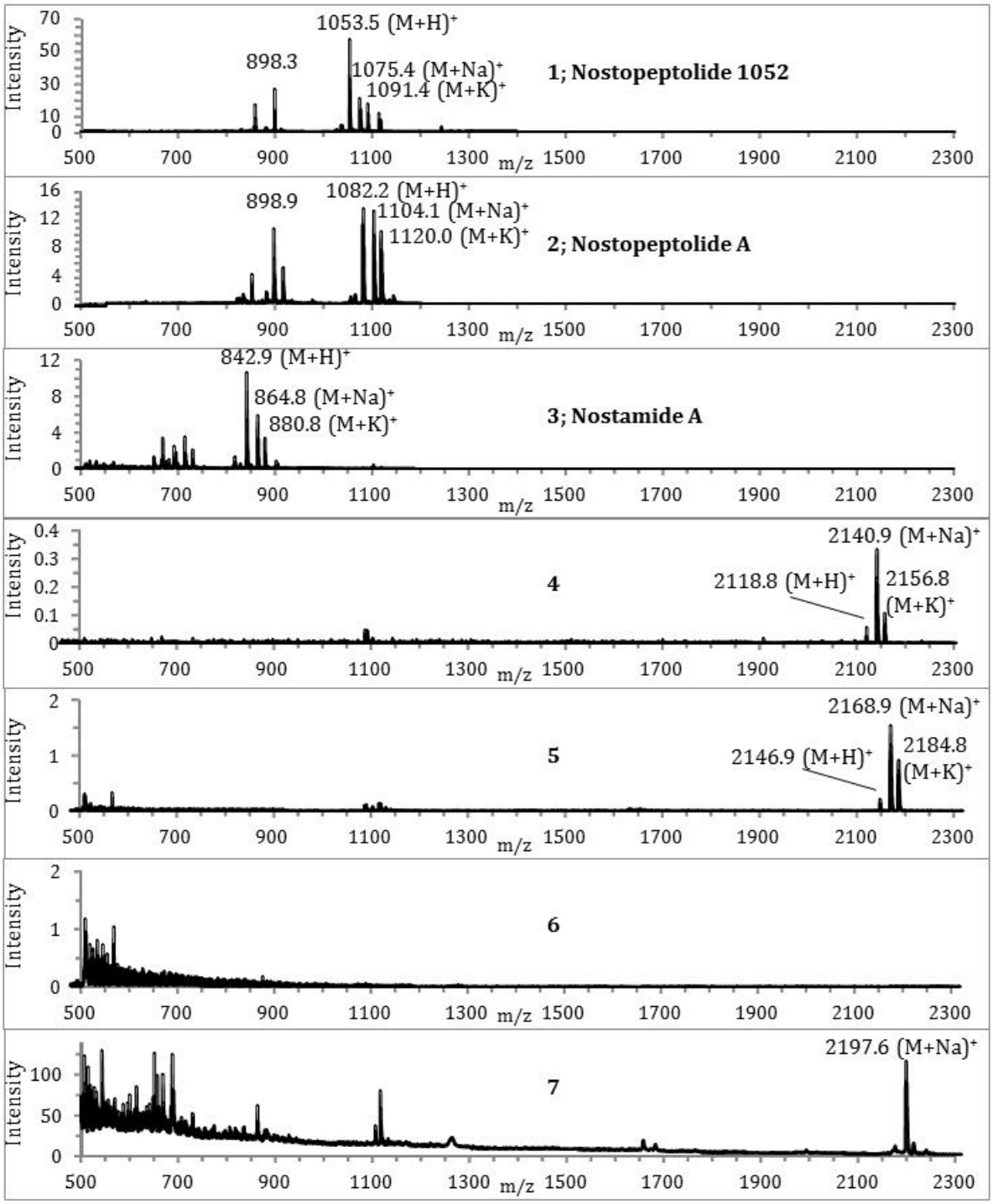

Figure S1 | MALDI TOF spectra for selected peaks of *N. punctiforme* PCC 73102 as shown in Figures 3 and 4. Peak numbers correspond to compound numbers in Fig. 3 and 4. Peaks 1 to 3 are shown as M+H, peaks 4, 5 and 7 contained metabolites with M=2117 Da, M=2145 Da and M=2173 Da, calculated from $M+Na^+$. Values for m/z are shown for the lightest isotope signal. Peaks 1 to 3 were identified as nostopeptolide 1052, A and nostamide A. See Fig. S2 for MS/MS fragmentation spectra. Both nostopeptolide peaks contained a cleavage fragment, indicative for their cyclic portion of M+H=898 Da.

Table S4. Observed PSD fragments of nostopeptolide 1052 and A for Figure S2.

Ion; *m/z* 1081(1053)	Observed fragment (Positive ion mode)
966(938)	Bu(Ac)-Ile-Ser-mPro-LeuAc-Leu-Gly-Asn-Tyr
898(898)	Ser-mPro-LeuAc-Leu-Gly-Asn-Tyr-Pro
829(829)	mPro-LeuAc-Leu-Gly-Asn-Tyr-Pro-OH
797(769)	Bu(Ac)-Ile-Ser-O-Pro-Tyr-Asn-Gly-Leu [-H_2O]
634(606)	Bu(Ac)-Ile-Ser(O-Pro)-mPro-LeuAc
551(551)	mPro-LeuAc-Leu-Gly-Asn
519(491)	Bu(Ac)-Ile-Ser-mPro-LeuAc [-H_2O]
451(451)	Pro-O-Ser-mPro-LeuAc
368(340)	Bu(Ac)-Ile-Ser-O-Pro
296(296)	Pro-Ser-mPro
267(267)	mPro-LeuAc/Leu-Gly-Asn [-H_2O]

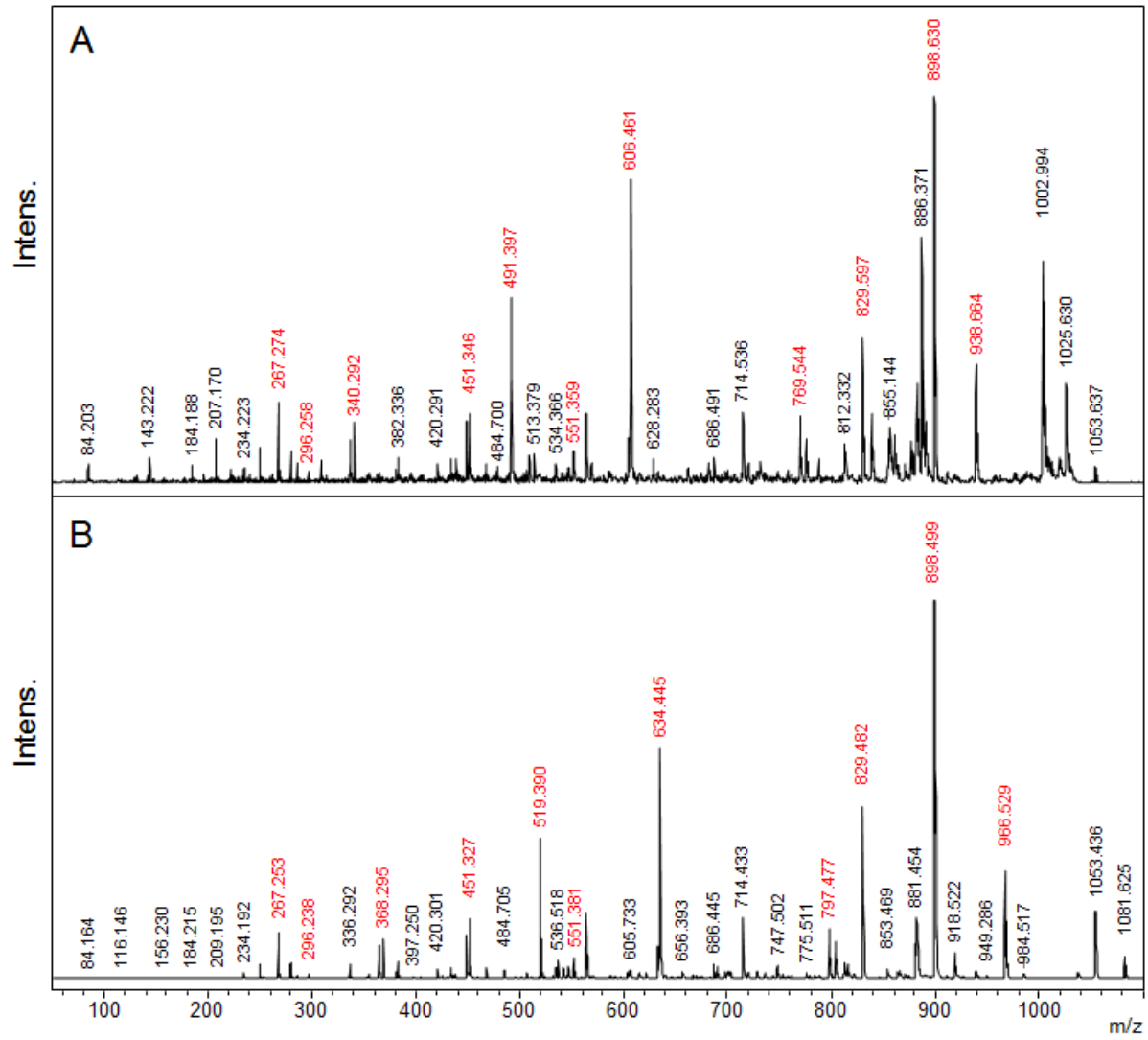

C

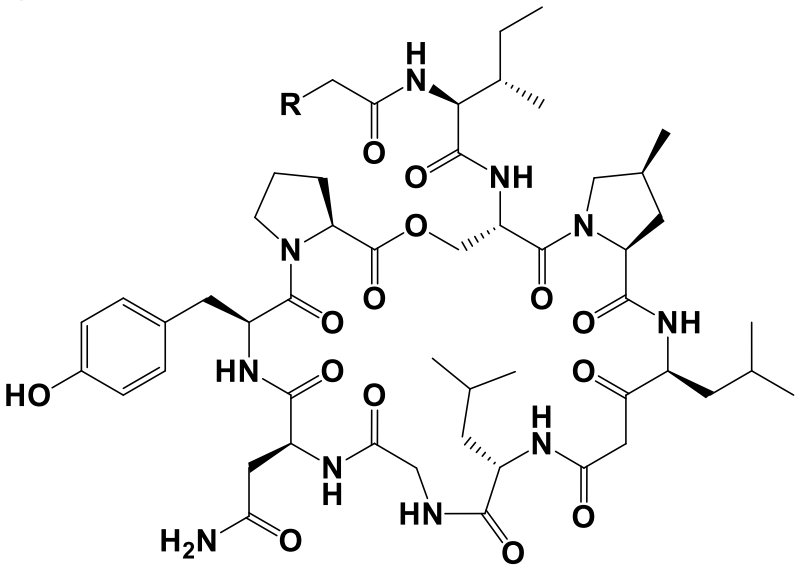

Nostopeptolide 1052 (R=H)
Nostopeptolide A (R=CH_2CH_3)

Figure S2. MALDI TOF PSD spectra (positive ion mode) of nostopeptolide 1052 (**A**) and nostopeptolide A (**B**). Structures of nostopeptolide 1052 and A (**C**). Red highlighted ions are assigned fragment ions as listed in Table S5.

Table S5. Observed PSD fragments of nostamide A for Figure S3.

Ion; *m/z* 842	Observed fragment (Positive ion mode)
814	**M**-CO
729	**M**-Ile
681	**M**-Hph
677	**M**-Phe
655	**M**-Hty
651	**M**-Phe-CO
594	**M**-MeGly-Hty
568	**M**-Ile-Hph
540	**M**-Ile-Hph-CO
523	Ile-Hph-MeGly-Hty
346	Ile-Php-MeGly
320	Phe-CO-Lys
275	Ile-Hph
249	MeGly-Hty
233	Hph-MeGly

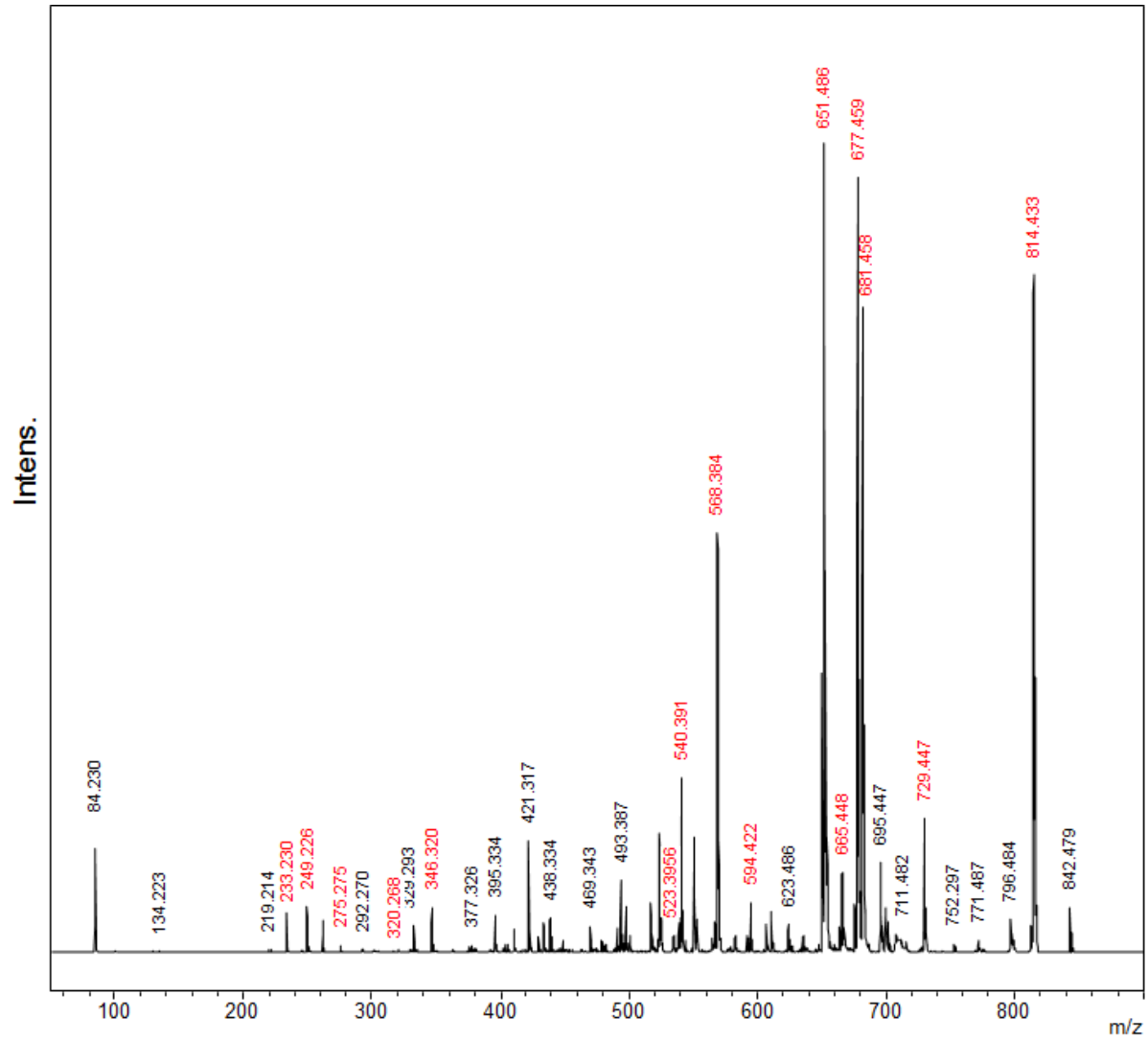

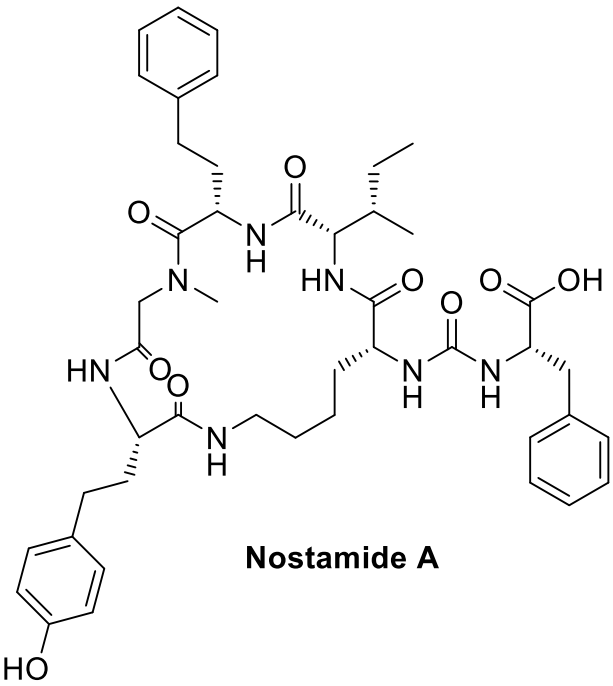

Figure S3. MALDI TOF PSD spectra (positive ion mode) of nostamide A. Structure of nostamide A. Red highlighted ions are assigned fragment ions as listed in Table S6.

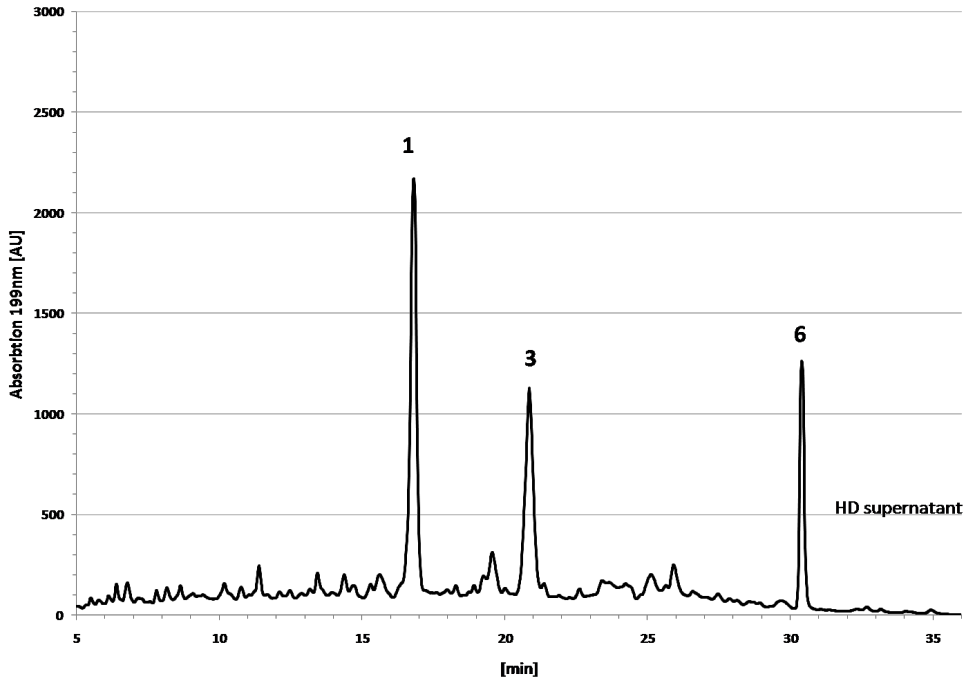

Figure S4 HPLC profile of the HD supernatant of *N. punctiforme* PCC 73102 obtained at day 17 of HD cultivation and used for the treatment of C+HD cultures. Compound numbers relate to peak numbers shown in Figures 3 and 4 and Figures S1-S3.

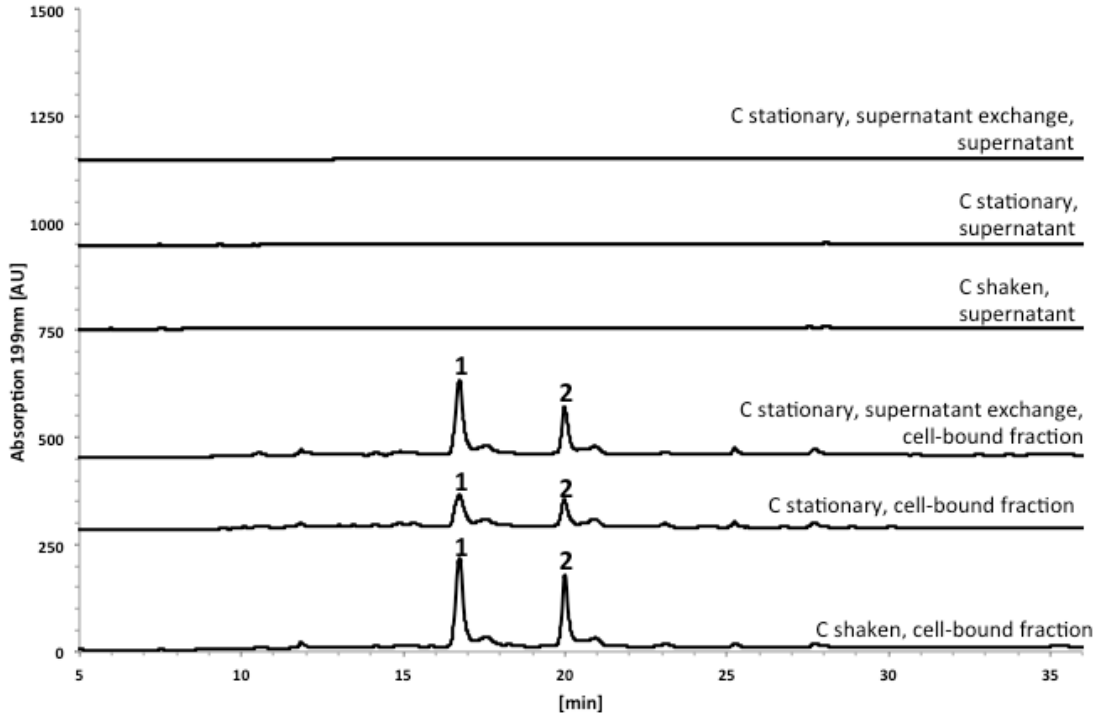

Figure S5 HPLC profiles of cellular extracts and supernatants of *N. punctiforme* PCC 73102 grown either as conventional stationary culture (C stationary) or as conventional shaken culture (C shaken) for 24d with or without supernatant exchange (supernatant was obtained by centrifugation at day 17 and re-added to the same culture). Neither mechanical shaking now mechanical supernatant exchange had a significant influence on the metabolites produced or secreted. Numbers relate to compound numbers in Figure 3 and 4. **1**: nostopeptolide 1052, **2**: nostopeptolide A

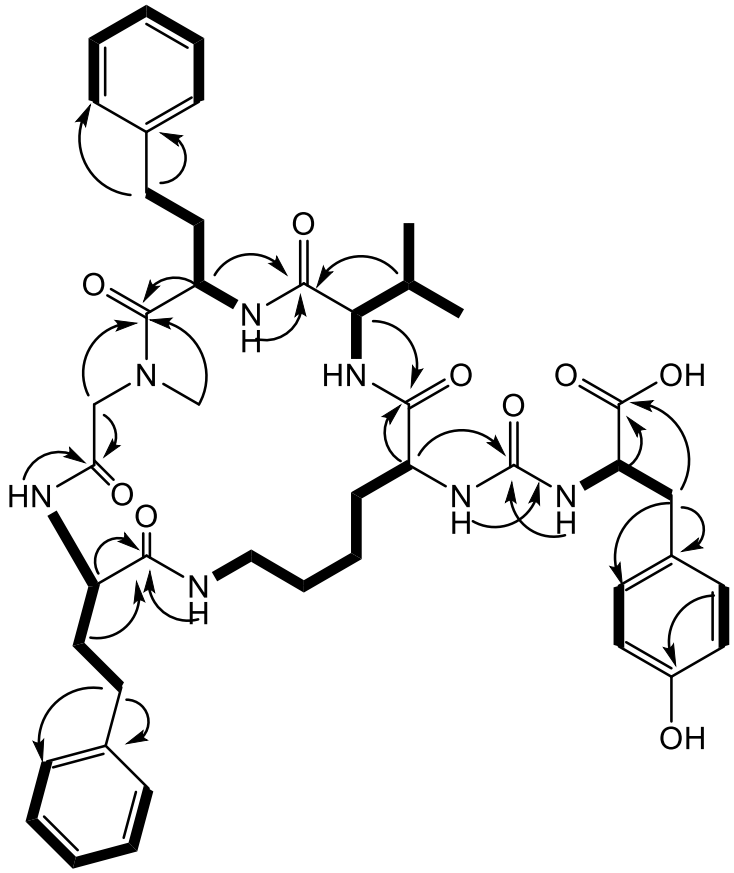

Figure S6. The key HMBC (arrow) and ^{1}H-^{1}H COSY (bold line) correlations of anabaenopeptin KVJ827.

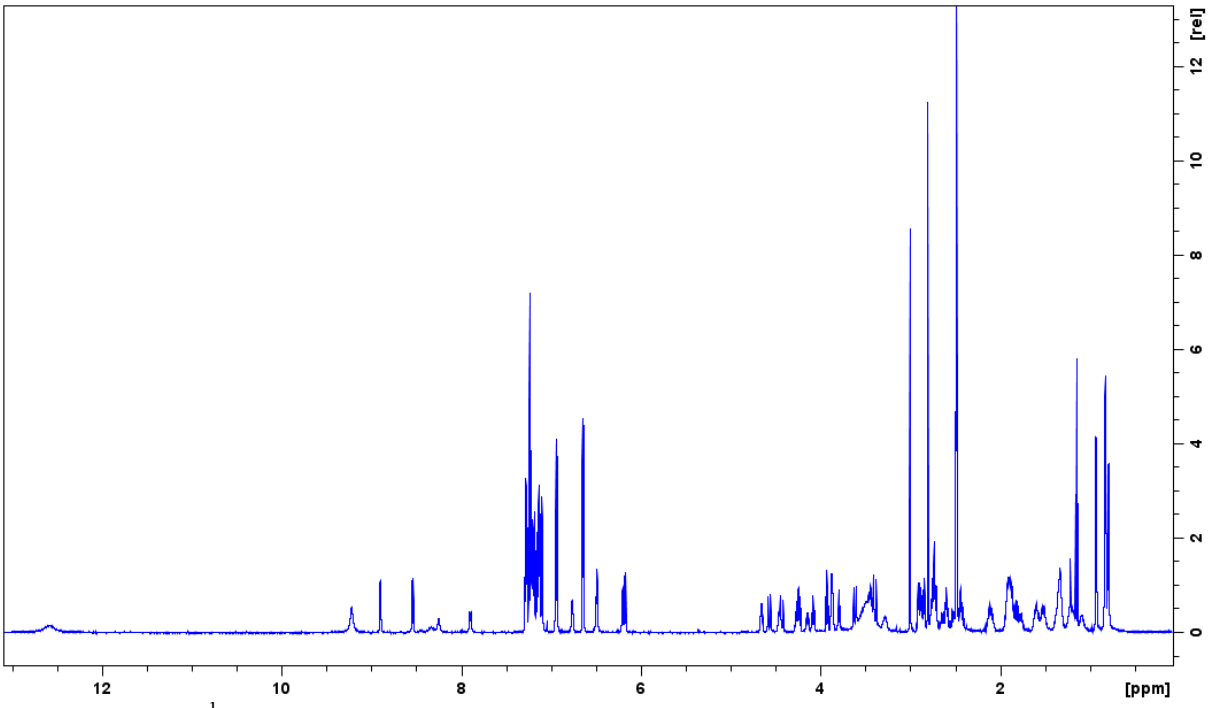

Figure S7. The ^{1}H NMR spectrum of anabaenopeptin KVJ827 in DMSO-d_6.

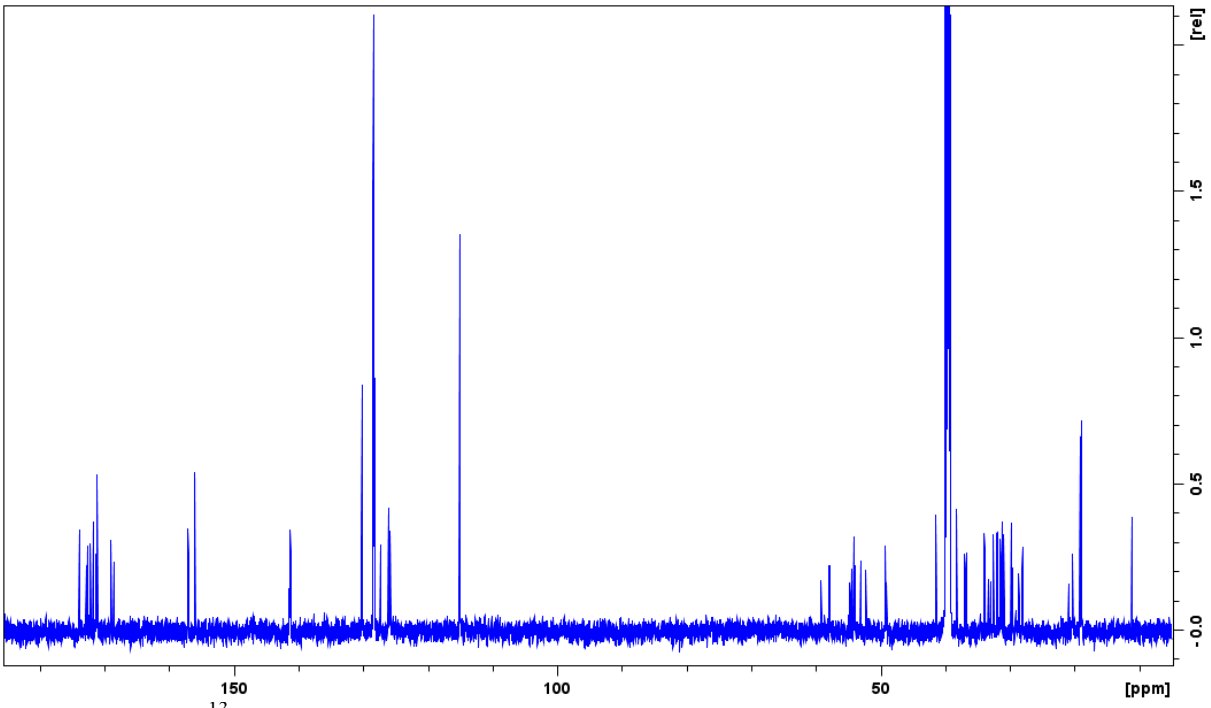

Figure S8. The ^{13}C NMR spectrum of anabaenopeptin KVJ827 in DMSO-d_6.

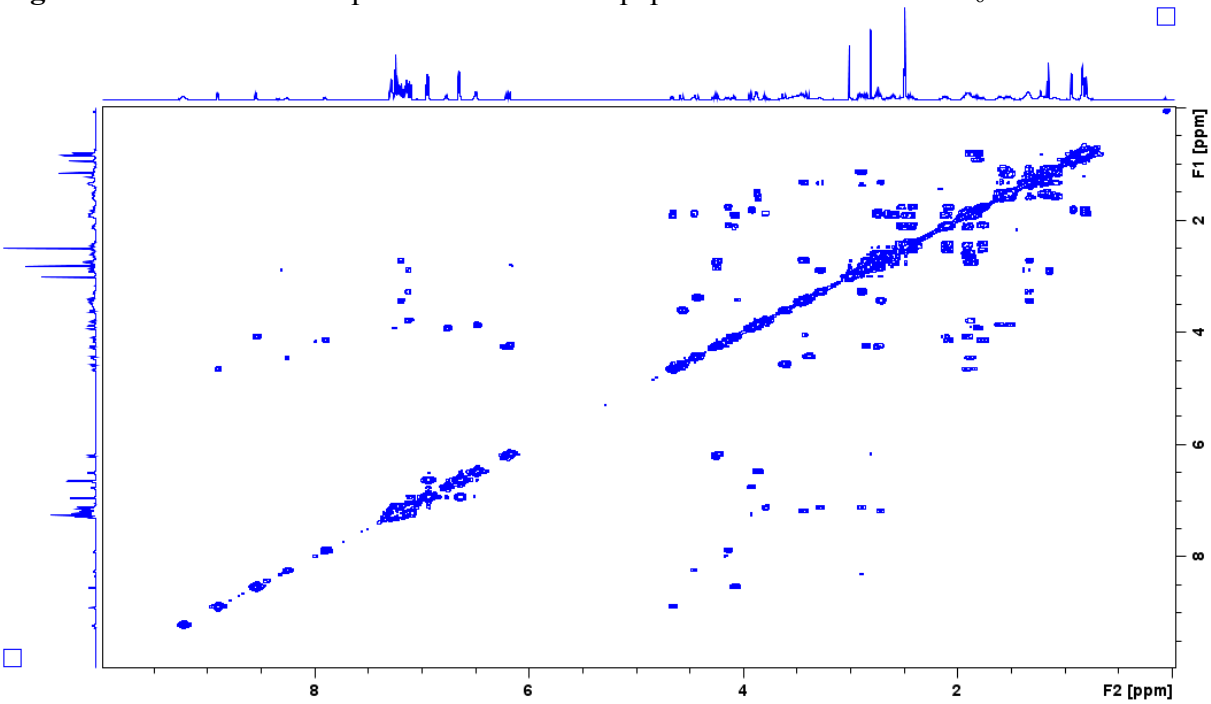

Figure S9. The ^{1}H-^{1}H COSY spectrum of anabaenopeptin KVJ827 in DMSO-d_6.

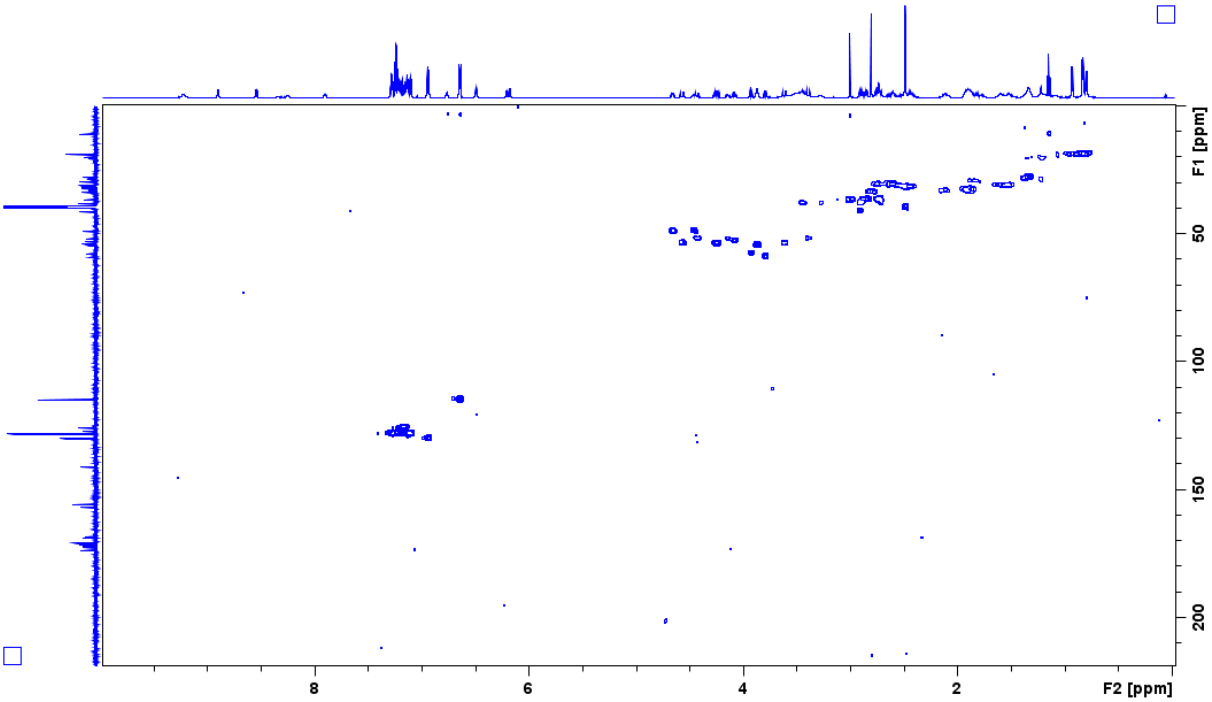

Figure S10. The HSQC spectrum of anabaenopeptin KVJ827 in DMSO-d_6.

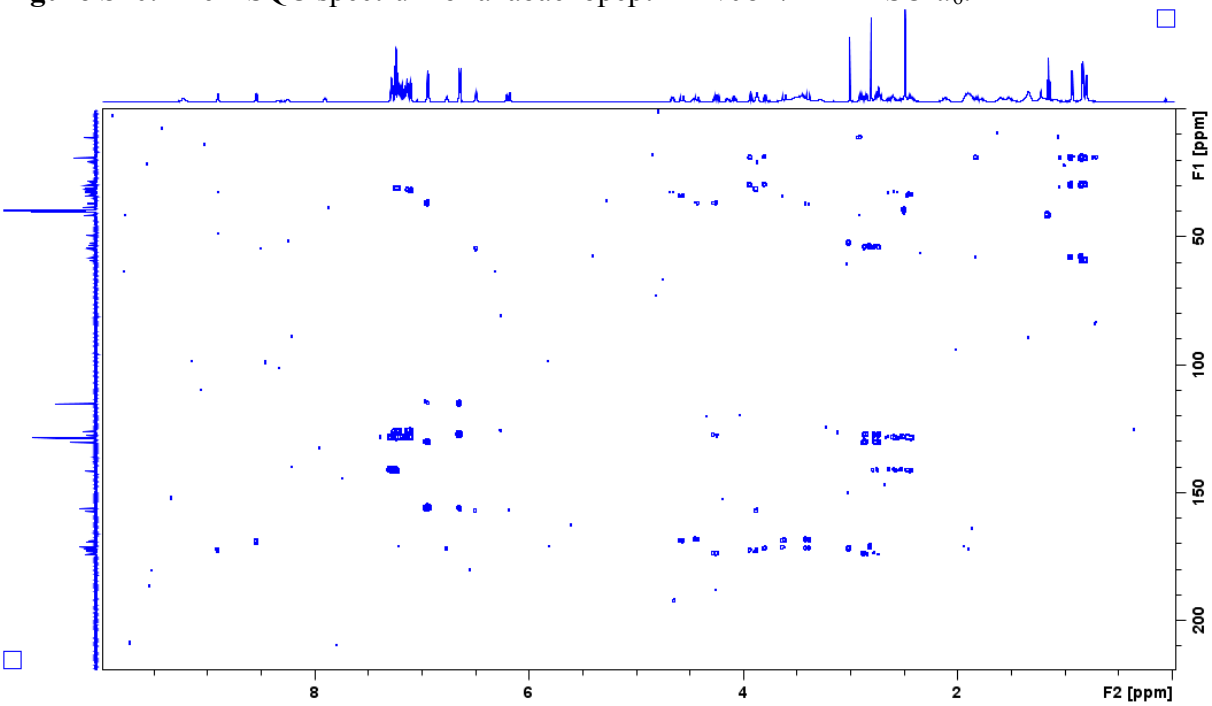

Figure S11. The HMBC spectrum of anabaenopeptin KVJ827 in DMSO-d_6.

Table S6. Observed fragments for Figure S12.

Label in **Figure S9**	Observed fragment (Positive ion mode)
A	**M**-CO
B	**M**-COO
C	**M**-Val or –Ile
D	**d**-CO
E	**M**-Hph
F	**M**-Phe or –Tyr
G	**f**-CO
H	**M**-Val(Ile)-Hph1
I	**h**-H_2O
J	**h**-CO
K	**i**-CO
L	**M**-Val(Ile)-Hph1-MeGly
M	Val(Ile)-Hph1-MeGly-Hph2
N	**M**-Hph1-MeGly-Hph2
O	Hph1-MeGly-Hph2
P	MeGly-Hph2-Lys
Q	Val(Ile)-Hph1-MeGly
R	Val(Ile)-Hph1
S	Hph1-MeGly/MeGly-Hph2
T	**s**-H_2O
U	Hph1/2-CO
V	Lys-CO-NH

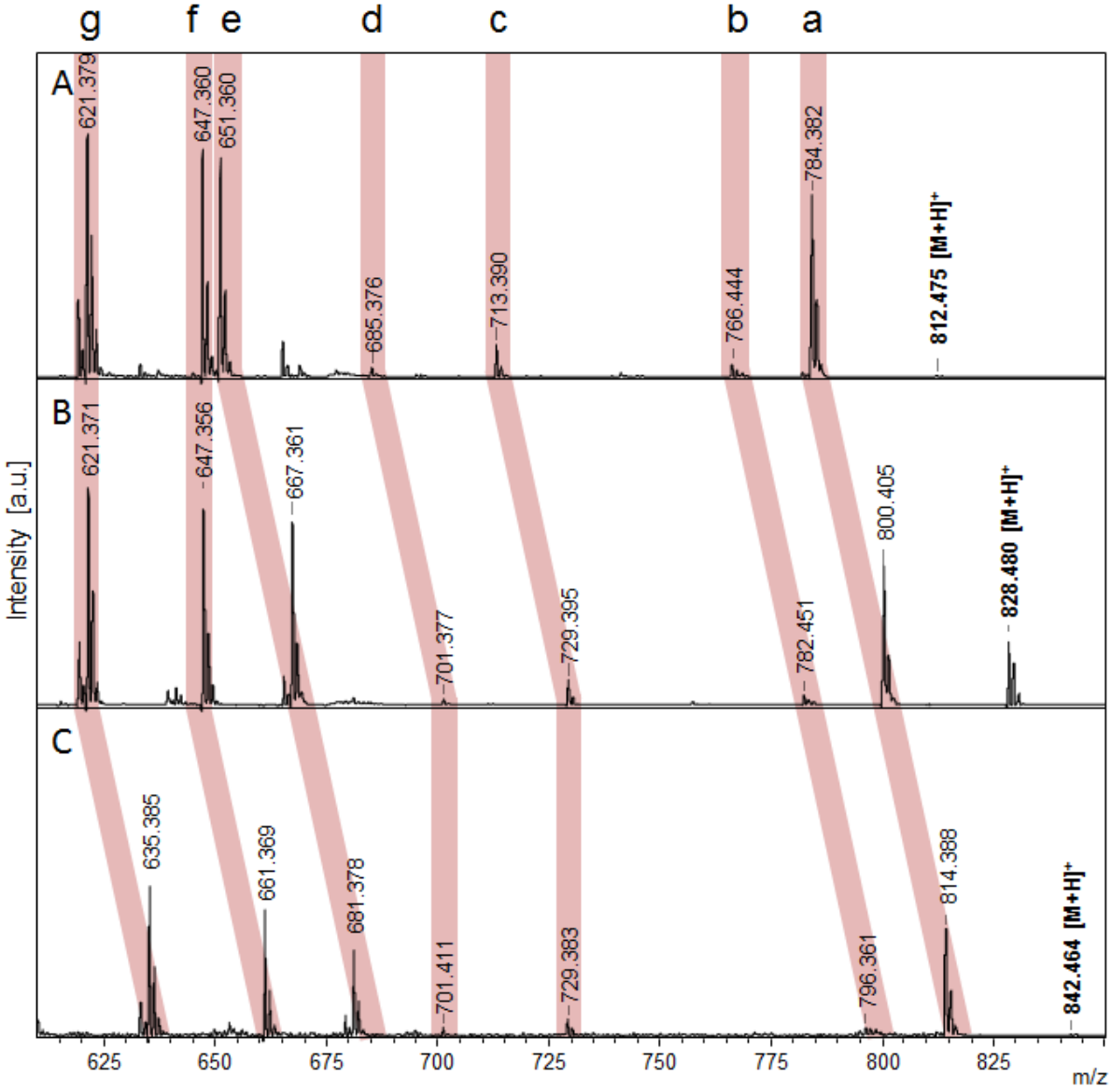

Figure S12. The MALDITOFMS PSD spectra of anabaenopeptin KVJ827, KVJ841, KVJ811. anabaenopeptin KVJ811 (A), KVJ827 (B), and KVJ841 (C). Observed ions as listed in Table S5 are highlighted in pink.

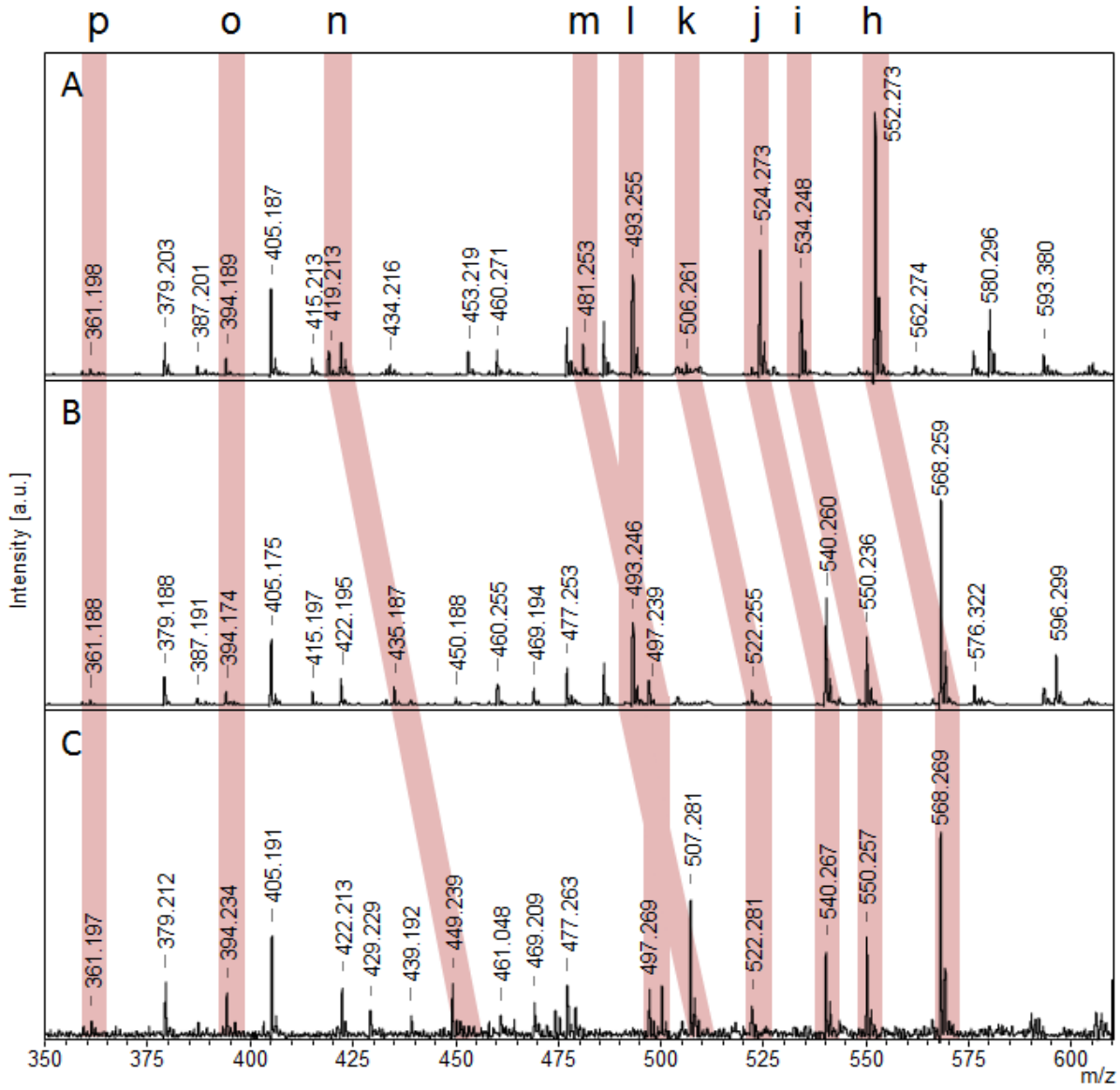

Figure S12. Continuation.

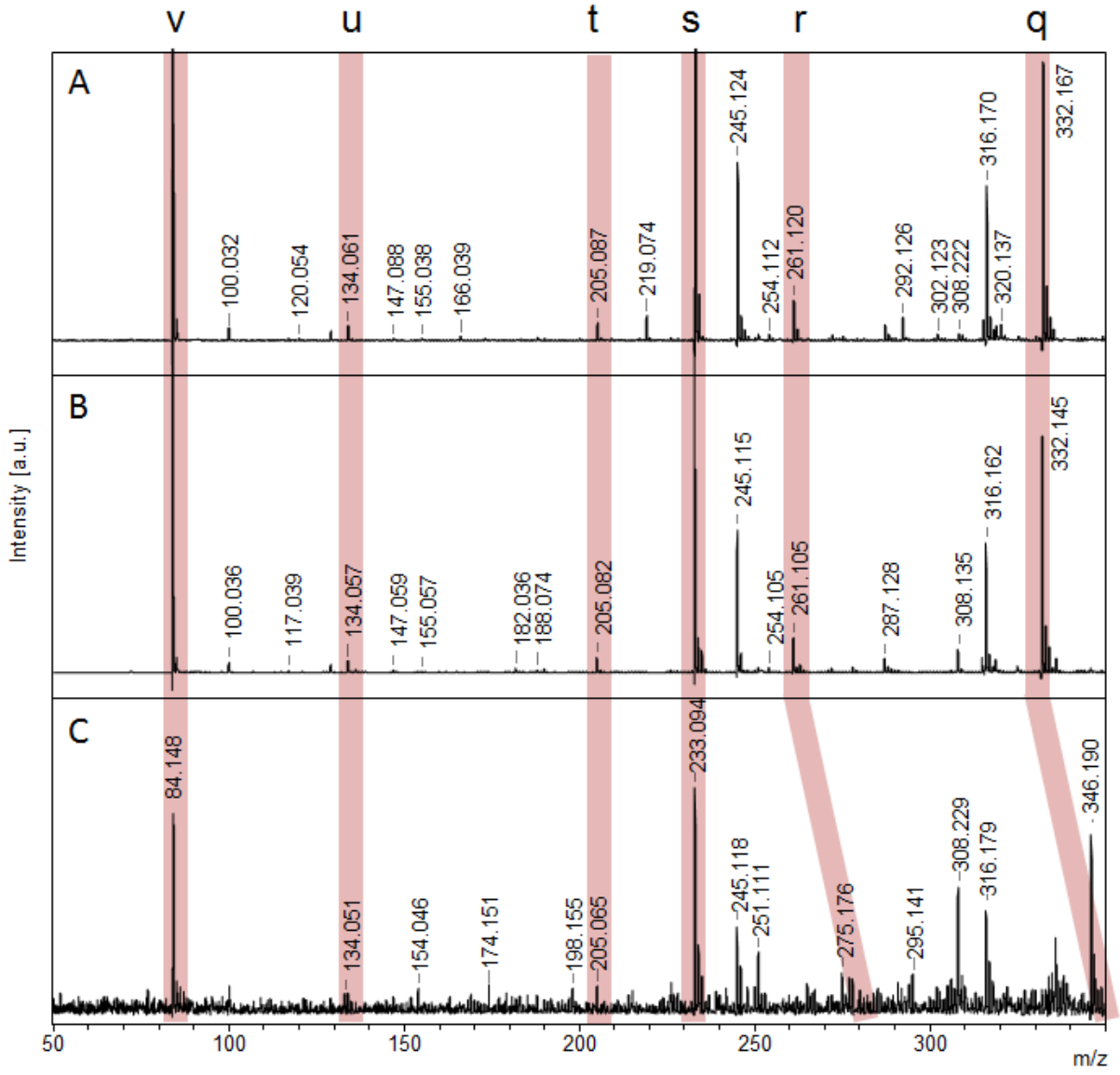

Figure S12. Continuation.

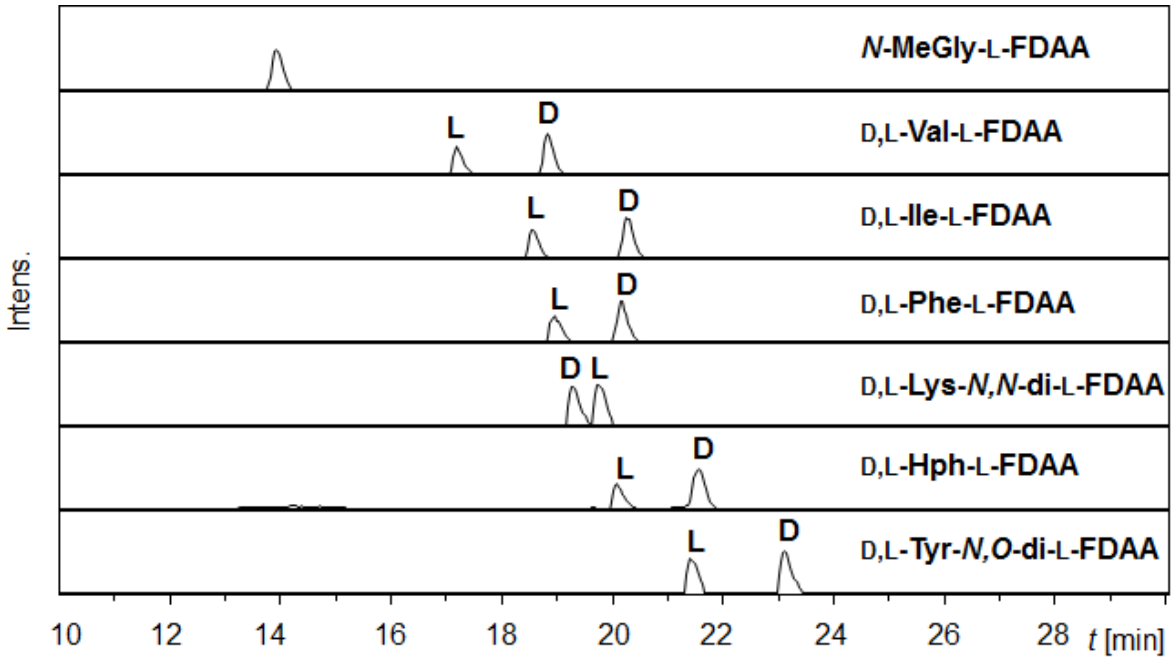

Figure S13. Extracted ion chromatogram (EIC) at negative ion mode of FDAA derivatives of standard amino acids by HPLC-MS. Data profile shows EIC as follows. *N*-MeGly-L-FDAA; *m/z* 341.8±0.5 $(M-H)^-$, D,L-Val-L-FDAA; *m/z* 369.7±0.5 $(M-H)^-$, D,L-Ile-L-FDAA; *m/z* 383.5±0.5 $(M-H)^-$, D,L-Phe-L-FDAA; *m/z* 417.3±0.5 $(M-H)^-$, D,L-Lys-*N*,*N*-di-L-FDAA; *m/z* 649.6±0.5 $(M-H)^-$, D,L-Hph-L-FDAA; *m/z* 431.4 $(M-H)^-$, D,L-Tyr-*N*,*O*-di-L-FDAA; *m/z* 684.4±0.5 $(M-H)^-$. Hph; homophenylalanine.

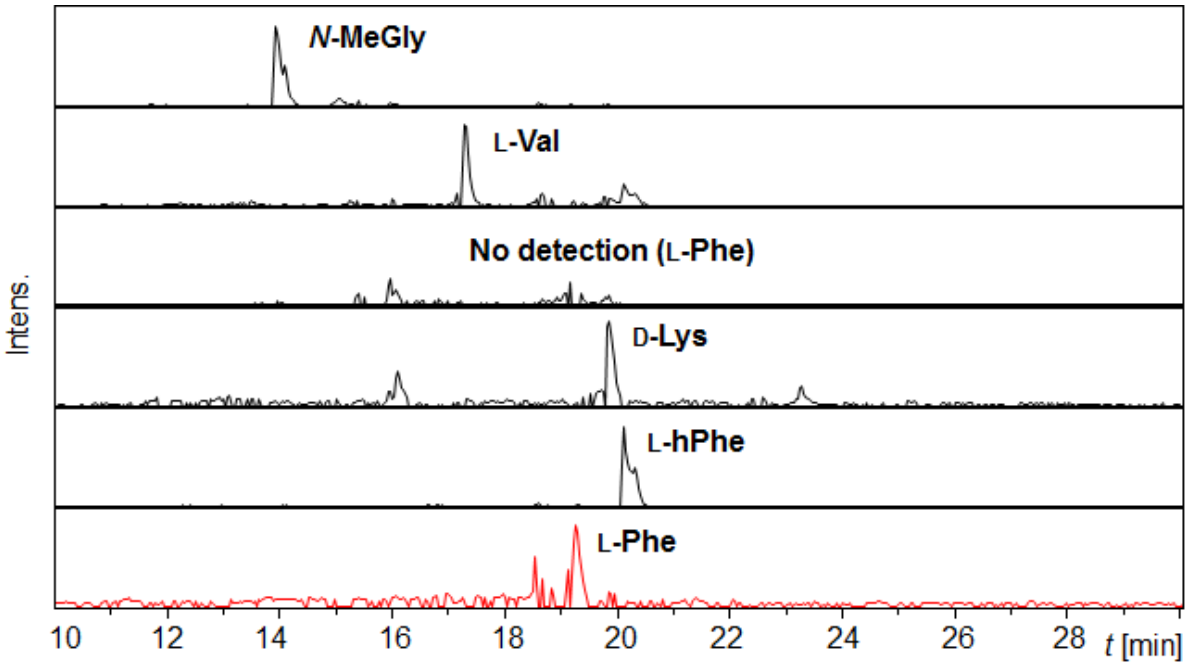

Figure S14. Extracted ion chromatogram at negative ion mode of FDAA derivatives of acid hydrolysate of anabaenopeptin KVJ811 (**10**) by HPLC-MS. L-Phe was initially not detected as the ureido bond was not hydrolysed by 6M HCl. To circumvent the problem, **10** was also hydrolyzed by hydrazine and derivatized by L-FDAA (red chromatogram). Data profile shows EIC as shown above figure S10.

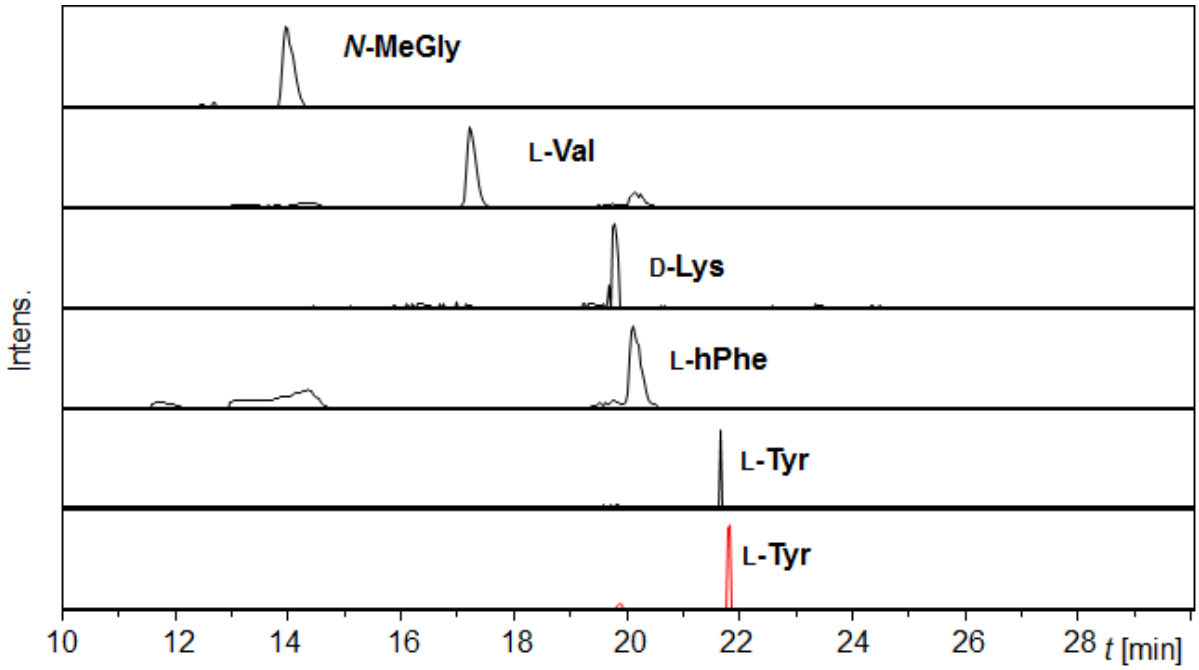

Figure S15. Extracted ion chromatogram at negative ion mode of FDAA derivatives of acid hydrolysate of anabaenopeptin KVJ827 (**8**) by HPLC-MS. As the ureido bond is often not hydrolysed by 6M HCl, **8** was also hydrolyzed by hydrazine and derivatized by L-FDAA (red chromatogram). Data profile shows EIC as shown above figure S10.

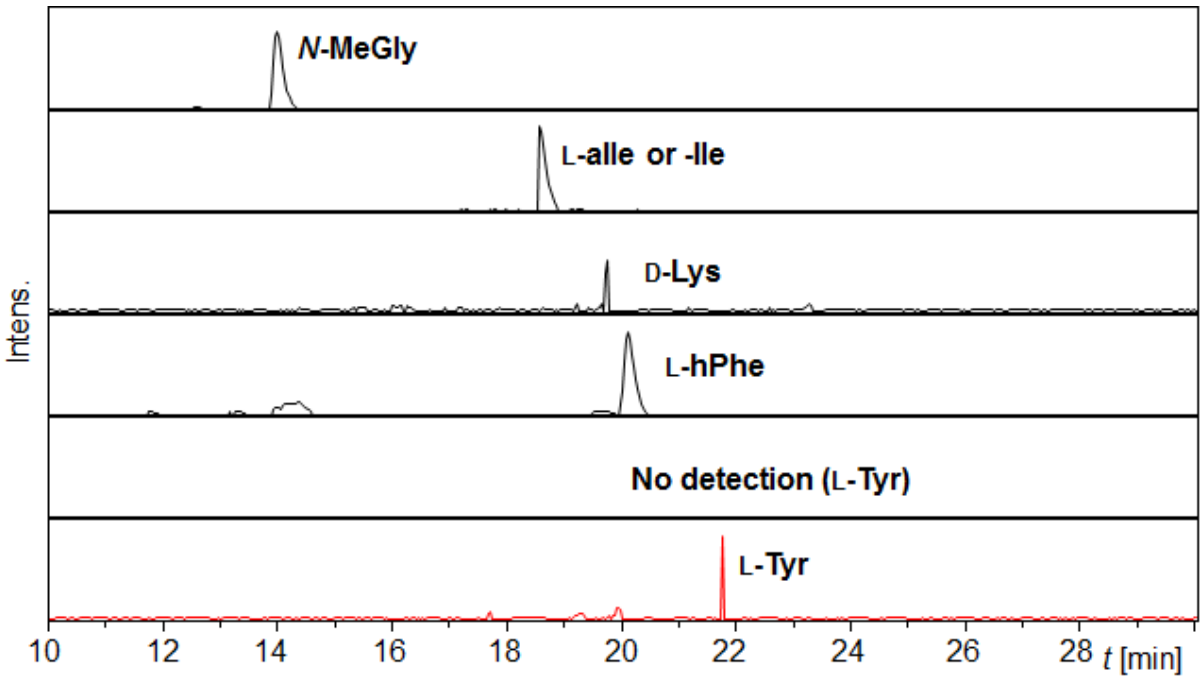

Figure S16. Extracted ion chromatogram at negative ion mode of FDAA derivatives of acid hydrolysate of anabaenopeptin KVJ841 (**9**) by HPLC-MS. L-Tyr was initially not detected as the ureido bond was not hydrolysed by 6M HCl. To circumvent the problem, **9** was also hydrolyzed by hydrazine and derivatized by L-FDAA (red chromatogram). The stereochemistry of Ile was not elucidated by this method. Further stereochemistry determination shows Figure S14. Data profile shows EIC as shown above figure S10.

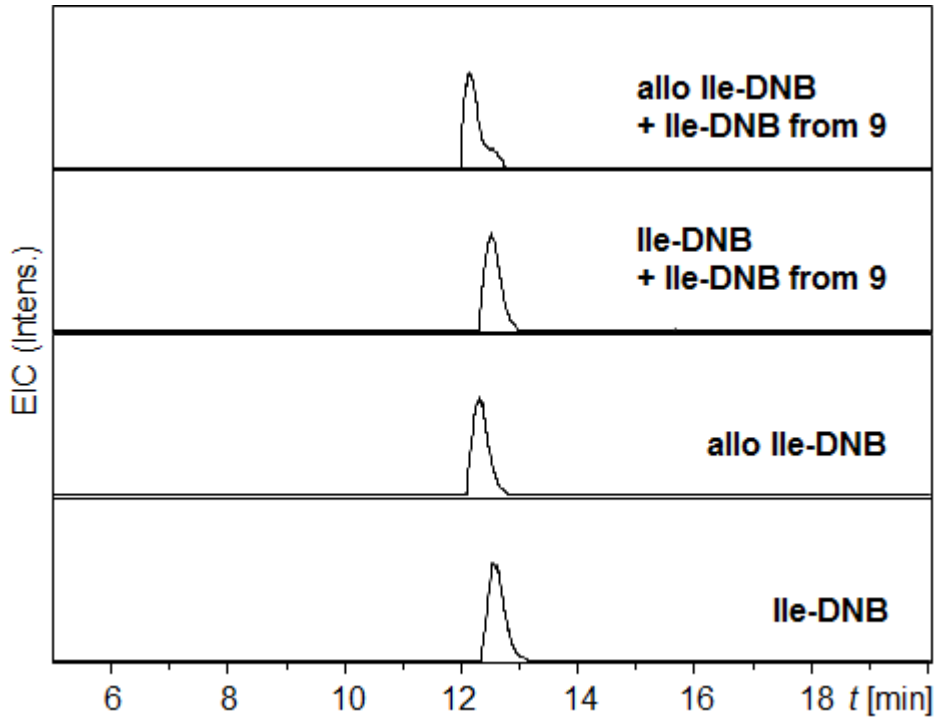

Figure S17. Stereochemistry determination of Ile in anabaenopeptin KVJ841 (**9**) by using Sanger reagent DNFB (1-fluoro-2,4-dinitrobenzene). Extracted ion chromatogram of DNB (dinitrobenzene) derivatives of standard amino acids and acid hydrolysate of **9** at *m/z* 383.5±0.5 (M-H) corresponding to Ile-DNB. Top 2 chromatograms show coinjections of acid hydrolysate of 9 and amino acid standards and bottom 2 chromatograms show amino acid standard derivatives, only. This method determined Ile of **9** is L-Ile.